Heliyon 9 (2023) e22089

Contents lists available at ScienceDirect

Heliyon

journal homepage: www.cell.com/heliyon

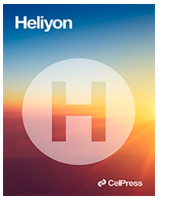

Qizhu Anti-Cancer Recipe promotes anoikis of hepatocellular carcinoma cells by activating the c-Jun N-terminal kinase pathway

Zhiyi Han [a,b], Qi Huang [a], Minling Lv [a], Mengqing Ma [a], Wei Zhang [a,b], Wenxing Feng [a,b], Rui Hu [a,b], Xinfeng Sun [a,b], Jing Li [a], Xin Zhong [a,b], Xiaozhou Zhou [a,b,*]

[a] *Department of Liver Disease, Shenzhen Traditional Chinese Medicine Hospital, No.1 Fuhua Road, Futian District, Shenzhen, 518000, China*
[b] *Department of Liver Disease, the Fourth Clinical Medical College of Guangzhou University of Chinese Medicine, No. 1 Fuhua Road, Futian District, Shenzhen, 518000, China*

ARTICLE INFO

Keywords:
Qizhu Anti-Cancer Recipe
Hepatocellular carcinoma
JNK
Anoikis resistance

ABSTRACT

Background: Qizhu Anti-Cancer Recipe (QACR) is a traditional Chinese medicine widely used in treating several liver diseases. However, its function and the relevant mechanism underlying its effect in treating hepatocellular carcinoma (HCC) remain unknown. The aim of this study was to explore the effect of QACR in HCC, which are expected to be a potential therapeutic scheme for HCC.

Materials and methods: The chemical compositions of QACR were determined by liquid chromatography/quadrupole time-of-fight mass spectrometry (LC-QTOF-MS). The anoikis-resistant HCC cell proliferation and angiopoiesis were detected using the cell counting kit 8 (CCK8) assay, trypan blue, calcein AM/EthD-1, flow cytometer, Western blot, and tube formation assays. An orthotopic xenograft mouse model was established to evaluate the *in vivo* effects of the QACR. The expression of proliferating cell nuclear antigen (PCNA), Bcl-2, CD31, caspase-3, caspase-8, caspase-9, PARP-1, DFF40, phospho-*c*-Jun NH2-terminal kinase (*p*-JNK), and JNK was assessed using Western blot and immunohistochemical analysis.

Results: QACR reduced the growth and tube formation of anoikis-resistant HCC cells and enhanced cell apoptosis *in vitro*. In the orthotopic xenograft mouse models, QACR suppressed the tumorigenesis of HCC *in vivo*. Mechanistically, QACR modulated the JNK pathway. The JNK inhibitor (SP600125) reverses the inhibitory effects of QACR on anoikis-resistant HCC cell proliferation and angiopoiesis.

Conclusion: Our study suggests that QACR suppresses the proliferation and angiopoiesis of anoikis-resistant HCC cells by activating the JNK pathway. Therefore, QACR is a promising new therapeutic strategy for treating hepatocellular carcinoma.

1. Introduction

Hepatocellular carcinoma (HCC), the primary tumor of the liver, is the sixth most prevalent cancer and the second leading cause of

* Corresponding author. Department of Liver Disease, Shenzhen Traditional Chinese Medicine Hospital, No. 1 Fuhua Road, Futian District, Shenzhen, 518000, China.
E-mail address: zxz1006@gzucm.edu.cn (X. Zhou).

https://doi.org/10.1016/j.heliyon.2023.e22089
Received 17 August 2023; Received in revised form 31 October 2023; Accepted 3 November 2023
Available online 13 November 2023
2405-8440/© 2023 The Authors. Published by Elsevier Ltd. This is an open access article under the CC BY-NC-ND license (http://creativecommons.org/licenses/by-nc-nd/4.0/).

cancer-related mortality worldwide [1]. According to data from *Global Cancer Statistics 2020*, HCC accounted for about 906,000 new cases and 830,000 deaths globally in 2020 [2]. Despite significant advances in therapeutic approaches, including local ablative therapy, surgical resection, and liver transplantation, the overall survival rate of patients with HCC remains unsatisfactory due to high recurrence and metastasis rates [3,4]. Therefore, understanding the molecular mechanisms underlying HCC pathogenesis could help develop novel strategies to improve the prediction, prevention, and treatment of HCC.

Anoikis is programmed cell death caused by cells separating from the extracellular matrix (ECM) or neighboring cells. Anoikis is a crucial defence mechanism against adherent-independent cell proliferation or reattachment to new matrices, inhibiting the colonisation of distant organs [5,6]. Tumor cells can acquire anoikis resistance, enabling them to survive during local dissemination, systemic circulation, and distant colonisation [3,7]. Acquiring anoikis resistance is an important prerequisite for intra-hepatic spread and extra-hepatic metastasis of HCC [8]. Additionally, anoikis-resistant tumor cells overexpress endothelial growth factor A (VEGFA) and display angiogenesis compared with their parental cells, which is necessary for anoikis-resistant cells to metastasise [7,9]. Therefore, the mechanistic role of anoikis in HCC needs to be investigated and could be important in developing effective new therapeutic strategies.

Currently, sorafenib is the only first-line systemic therapy recommended for advanced HCC [10]. Previous studies have demonstrated that sorafenib exerts its anticancer effect by inducing apoptosis and inhibiting the growth and angiogenesis of HCC cells [11]. However, due to its low response rate (2 %) and a poor prognosis (5.5 months) [12], new therapies for HCC are urgently needed. Traditional Chinese medicine (TCM) is a distinct diagnostic and therapeutic approach with a long history [13]. Studies have reported that TCM was effective in treating cancer [14]. For example, Dihydroartemisinin exerts anti-angiogenic effects during tumor growth through inducing anoikis of endothelial cell by activating the c-Jun N-terminal kinase (JNK) signaling pathway [15]. Moreover, Extracts of Qizhu decoction inhibit hepatitis and hepatocellular carcinoma *in vitro* and in C57BL/6 mice by suppressing NF-κB signaling [16]. Qizhu Anti-Cancer Recipe (QACR) is a Chinese herbal compound extracted from ten species of medicinal herbs: *Bupleurum root, Radix Paeoniae Alba, Curcuma zedoaria, Astragalus membranaceus, Radix Glycyrrhizae, Roasted rhizoma atractylodis macrocephalae, semen coicis, Common Yam Rhizome, Spreading Hedyotis Herb, and Endothelium Corneum Gigeriae Galli (ECGG) extract*. ECGG is a traditional Chinese drug consisting of the dried gizzard membrane of *Gallus gallus domesticus Brisson*. With potent liver-dredging and stasis-dispersing effects, QACR is a potential resource for creating novel HCC medications. However, experimental research investigating the therapeutic potential of HCC remains scarce. In addition, the molecular mechanisms underlying the effect of QACR in tumorigenesis and metastasis remain largely unknown.

The c-Jun N-terminal kinase (JNK), belonging to the MAPK family (also known as stress-activated protein kinase SAPK), is activated in response to various stimuli, such as infection, oxidative stress, cytotoxic drugs, cytoskeletal changes and DNA damage [17]. Xu et al. reported that inhibiting JNK expression reversed MT189-mediated inhibition of endothelial proliferation, migration, differentiation, and angiogenesis [18]. In colorectal cancer, norcantharidin induces cell anoikis by activating the JNK signaling pathway [19]. Its role and the corresponding downstream signaling in liver cancer need to be further explored. This study investigated whether QACR suppresses the proliferation, metastasis, and angiopoiesis of anoikis-resistant HCC cells. The mechanism underlying the efficacy of the QACR in treating HCC was identified.

2. Material and methods

2.1. Cell culture

HCC cell lines (MHCC97-L and SK-Hep-1) and HUVECs were purchased from Jennio Biotech (Guangzhou, China). The HCC cell lines and HUVECs were cultured in Dulbecco's modified Eagle medium (DMEM) (Life Technologies, Gaithersburg, USA) supplemented with 10 % fetal bovine serum (FBS) (Sigma Aldrich, St. Louis, MO, USA), 100 U/mL penicillin (Life Technologies, Carlsbad, CA, USA), and 100 μg/ml streptomycin (Life Technologies, Carlsbad, CA, USA). The cells were maintained in a humidified chamber at 37 °C under 5 % CO_2.

2.2. In vivo model of anoikis

All *in vivo* experiments were performed according to the Care and Use of Laboratory Animals guidelines of Peking University Shenzhen Graduate School. This study was approved by the Institutional Animal Care and Use Committee (IACUC) of Peking University Shenzhen Graduate School (Approval No. 92153). MHCC97-L cells infected with lentivirus encoding luciferase gene were implanted into the left hepatic lobe of BALB/c male nude mice (four-week-old). After 4 weeks of implantation, tumor development was monitored using a bioluminescence imaging system (IVIS Lumina XR, Caliper, USA). All mice were randomly assigned to five groups (6 mice per group) and treated once daily by intragastric injection as follows: The control group was treated with saline solution; the low-dose group was treated with 10.4 g/kg of Anti-Cancer Recipe; the middle-dose group was treated with 20.8 g/kg of Anti-Cancer Recipe; the high-dose group was treated with 41.6 g/kg of Anti-Cancer Recipe; and the positive group was treated with 0.096 g/kg of sorafenib. After 30 days of intragastric injection, tumor growth was evaluated using a bioluminescence imaging system (IVIS Lumina XR). After mice were sacrificed, tumor tissues from the liver were harvested for hematoxylin and eosin (H&E) staining and immunohistochemical analysis.

Table 1
Active compounds of Qizhu Anti-Cancer Recipe.

Name	Formula	Calc. MW	RT [min]	mzCloud Best Match	MS2	Reference Ion
Oleanolic acid	C30H48 O3	456.35978	22.171	100	DDA for preferred ion	[M + H–H2O]+1
Adenosine	C10H13 N5 O4	267.09632	4.484	99.9	DDA for preferred ion	[M+H]+1
D-(+)-Proline	C5 H9 N O2	115.06353	1.392	99.9	DDA for preferred ion	[M+H]+1
Daidzein	C15H10 O4	272.06849	14.131	99.9	DDA for other ion	[M-H-H2O]-1
Formononetin	C16H12 O4	286.08423	14.63	99.9	DDA for other ion	[M-H-H2O]-1
2,3,4,9-Tetrahydro-1H-β-carboline-3-carboxylic acid	C12H12 N2 O2	216.08967	8.55	99.9	DDA for preferred ion	[M+H]+1
L-Phenylalanine	C9 H11 N O2	148.05236	5.232	99.9	DDA for other ion	[M + NH4]+ 1
Benzoic acid	C7 H6 O2	122.03551	9.714	99.9	DDA for preferred ion	[M − H]-1
Nicotinic acid	C6 H5 N O2	123.0323	2.014	99.8	DDA for preferred ion	[M+H]+1
2,3-Dihydro-1-benzofuran-2-carboxylic acid	C9 H8 O3	164.04626	11.477	99.8	DDA for preferred ion	[M − H]-1
Dibutyl phthalate	C16H22 O4	278.15128	18.582	99.7	DDA for preferred ion	[M+H]+1
Isoliquiritigenin	C15H12 O4	256.07289	11.893	99.7	DDA for preferred ion	[M+H]+1
Citraconic acid	C5 H6 O4	130.02551	5.756	99.7	DDA for preferred ion	[M − H]-1
Salicylic acid	C7 H6 O3	138.03047	12.997	99.6	DDA for preferred ion	[M − H]-1
4-Indolecarbaldehyde	C9 H7 N O	145.05151	11.863	99.6	DDA for preferred ion	[M − H]-1
Chlorogenic acid	C16H18 O9	372.10573	9.813	99.6	DDA for other ion	[M-H-H2O]-1
Genistin	C21H20 O10	432.10564	12.217	99.6	DDA for preferred ion	[M+H]+1
Trigonelline	C7 H7 N O2	137.04761	1.475	99.6	DDA for preferred ion	[M+H]+1
Ferulic acid	C10H10 O4	194.0574	11.837	99.6	DDA for preferred ion	[M − H]-1
Adenosine 5′-monophosphate	C10H14 N5 O7 P	347.0627	2.254	99.6	DDA for preferred ion	[M+H]+1
Salicylic acid	C7 H6 O3	138.03082	9.078	99.6	DDA for preferred ion	[M − H]-1
Di(2-ethylhexyl) phthalate	C24H38 O4	390.27599	23.072	99.6	DDA for preferred ion	[M+H]+1
DL-Homoserine	C4 H9 N O3	119.0584	1.335	99.6	DDA for preferred ion	[M+H]+1
4-Oxoproline	C5 H7 N O3	129.04133	2.648	99.5	DDA for preferred ion	[M − H]-1
Azelaic acid	C9 H16 O4	188.10405	13.419	99.5	DDA for preferred ion	[M − H]-1
5-Hydroxymethyl-2-furaldehyde	C6 H6 O3	126.0319	5.947	99.5	DDA for preferred ion	[M+H]+1
5′-S-Methyl-5′-thioadenosine	C11H15 N5 O3 S	297.08934	7.95	99.5	DDA for preferred ion	[M+H]+1
Bis(4-ethylbenzylidene)sorbitol	C24H30 O6	414.20369	17.619	99.5	DDA for preferred ion	[M+H]+1
Isoliquiritigenin	C15H12 O4	256.0731	13.682	99.4	DDA for preferred ion	[M+H]+1
(1r,3R,4s,5S)-4-{[(2E)-3-(3,4-dihydroxyphenyl)prop-2-enoyl] oxy}-1,3,5-trihydroxycyclohexane-1-carboxylic acid	C16H18 O9	354.09472	9.813	99.4	DDA for preferred ion	[M+H]+1
[(3R,5R,6S,8S)-3-(β-D-Glucopyranosyloxy)-6-hydroxy-8-methyl-9,10-dioxatetracyclo[4.3.1.02,5 03,8]dec-2-yl]methyl benzoate	C23H28 O11	480.16247	10.073	99.4	DDA for preferred ion	[M + FA-H]-1
Bis(4-ethylbenzylidene)sorbitol	C24H30 O6	414.20339	17.198	99.4	DDA for preferred ion	[M+H]+1
Ononin	C22H22 O9	430.12561	13.419	99.4	DDA for preferred ion	[M+H]+1

(*continued on next page*)

Table 1 (*continued*)

Name	Formula	Calc. MW	RT [min]	mzCloud Best Match	MS2	Reference Ion
L-Glutamic acid	C5 H9 N O4	147.05301	1.327	99.4	DDA for preferred ion	[M+H]+1
Daidzin	C21H20 O9	416.11059	11.252	99.4	DDA for preferred ion	[M+H]+1
(±)9,10-dihydroxy-12Z-octadecenoic acid	C18H34 O4	296.23521	19.468	99.4	DDA for preferred ion	[M − H]-1
Isoliquiritigenin	C15H12 O4	256.07292	11.487	99.4	DDA for preferred ion	[M+H]+1
{(3R,5R,6S,8S)-3-[(6-*O*-Benzoyl-β-D-glucopyranosyl)oxy]-6-hydroxy-8-methyl-9,10-dioxatetracyclo[4.3.1.02,5.03,8]dec-2-yl}methyl benzoate	C30H32 O12	584.18805	14.451	99.3	DDA for preferred ion	[M+H]+1
2′-*O*-Methyladenosine	C11H15 N5 O4	281.11235	5.937	99.3	DDA for preferred ion	[M+H]+1
Bis(4-ethylbenzylidene)sorbitol	C24H30 O6	414.20346	16.762	99.3	DDA for preferred ion	[M+H]+1
Quercetin	C15H10 O7	302.04201	11.649	99.3	DDA for preferred ion	[M+H]+1
7-hydroxy-3-(4-methoxyphenyl)-4H-chromen-4-one	C16H12 O4	268.07315	15.88	99.3	DDA for preferred ion	[M+H]+1
4-Coumaric acid	C9 H8 O3	164.04712	11.489	99.3	DDA for preferred ion	[M+H]+1
Daidzein	C15H10 O4	254.05753	14.136	99.3	DDA for preferred ion	[M+H]+1
Phenylacetaldehyde	C8 H8 O	120.05618	11.474	99.2	DDA for preferred ion	[M − H]-1
Formononetin	C16H12 O4	268.07285	13.383	99.2	DDA for preferred ion	[M + H + MeOH]+1
N6–Me-Adenosine	C11H15 N5 O4	281.11257	6.552	99.2	DDA for preferred ion	[M+H]+1
Palmitic acid	C16H32 O2	256.24027	22.667	99.2	DDA for preferred ion	[M − H]-1
Daidzein	C15H10 O4	272.06835	16.303	99.2	DDA for other ion	[M-H-H2O]-1
Gallic acid	C7 H6 O5	124.01498	5.208	99.2	DDA for other ion	[M + FA-H]-1
Isoliquiritigenin	C15H12 O4	256.07339	9.816	99.1	DDA for preferred ion	[M+H]+1
Methyl palmitate	C17H34 O2	287.28191	15.109	99.1	DDA for preferred ion	[M+H]+1
Isoliquiritigenin	C15H12 O4	256.07331	15.662	99.1	DDA for preferred ion	[M+H]+1
β-Muricholic acid	C24H40 O5	816.57539	18.936	99.1	DDA for preferred ion	[M − H]-1
2-(Acetylamino)hexanoic acid	C8 H15 N O3	173.10432	10.577	99.1	DDA for preferred ion	[M − H]-1
Anthranilic acid	C7 H7 N O2	137.04651	12.173	99	DDA for preferred ion	[M − H]-1
Quercetin-3β-D-glucoside	C21H20 O12	464.09514	12.12	99	DDA for preferred ion	[M+H]+1
3-{[(2S,3R,4S,5S,6R)-6-({[(2R,3R,4R)-3,4-dihydroxy-4-(hydroxymethyl)oxolan-2-yl]oxy}methyl)-3,4,5-trihydroxyoxan-2-yl]oxy}-2-methyl-4H-pyran-4-one	C17H24 O12	210.06329	7.375	99	DDA for other ion	[2 M + H]+1
Asperulosidic acid	C18H24 O12	449.15251	9.299	99	DDA for preferred ion	[M+H]+1
Glucose 1-phosphate	C6 H13 O9 P	260.02956	1.649	99	DDA for preferred ion	[M+H]+1
Quercetin-3β-D-glucoside	C21H20 O12	464.09487	11.649	99	DDA for preferred ion	[M+H]+1

2.3. Screening of active ingredients of Qizhu Anti-Cancer Recipe

The chemical composition of QACR was measured by liquid chromatography/quadrupole time-of-fight mass spectrometry (LC-QTOF-MS), All the reagents, including polydatin, corilagin, ethanol, and other reference standards, were obtained from Sigma-Aldrich (St. Louis, MO, USA). Active compounds of Qizhu Anti-Cancer Recipe are shown in Table 1.

2.4. The cell counting kit 8 assay

Cells were seeded in the ultra-low attachment 6-well plates (Corning Inc., Corning, NY, USA) overnight at a density of 2×10^5 per well. Then, they were treated with varying concentrations of Anti-Cancer Recipe. After 72h, 200 μl of cell counting kit 8 (CCK8) reagents (Sigma Aldrich, St. Louis, MO, USA) were added to each well and incubated for 3 h at 37 °C. The optical absorbance was measured at 450 nm using a Microplate Reader (Thermo Fisher Scientific, Waltham, MA, USA).

2.5. Trypan blue exclusion assay

MHCC97-L and SK-Hep-1 cells (2×10^5 per well) were seeded overnight in the ultra-low attachment 6-well plates (Corning Inc.). The cells were treated with 20 μg/ml, 40 μg/ml, and 200 μg/ml QACR or 3.72 μg/ml sorafenib. After 14 days, the cells were harvested and stained with 0.4 % trypan blue (Gibco BRL, Grand Island, NY, USA). The stained cells were analysed under a light microscope (Olympus Corp., Tokyo, Japan).

2.6. AM/ETHD-1 assay

Studies have shown that the calcein AM/EthD-1 dual-fluorescent dying assay can simultaneously stain live cells green and dead cells red. Briefly, MHCC97-L and SK-Hep-1 cells were cultured overnight in the ultra-low attachment 6-well plates (Corning Inc.). Then, they were treated with 20 μg/ml, 40 μg/ml, and 200 μg/ml QACR or 3.72 μg/ml sorafenib for 14 days. To dilute serum-containing esterase that may cause false positives, 100 μl of PBS was added into each well to wash the cells. Thereafter, 0.5 ml of dual fluorescence calcein AM/EthD-1 assay reagents were added to each well and incubated at room temperature for 15 min. Samples were examined using a FACSAria II flow cytometer (BD Biosciences, San Jose, CA, USA).

2.7. Flow cytometry assay of apoptosis

MHCC97-L and SK-Hep-1 cells were seeded overnight in the ultra-low attachment 6-well plates (Corning Inc.). Then, the cells were treated with 20 μg/ml, 40 μg/ml, and 200 μg/ml QACR or 3.72 μg/ml sorafenib for 14 days. Next, the cells were harvested, washed twice with PBS, and resuspended in 200 μL binding buffer. Afterward, cells were stained with 5 μL of annexin V (0.5 mM/L) and 5 μL propidium iodide (1 μg/ml). The cells were examined using a FACSAria II flow cytometer (BD Biosciences).

2.8. Western blot

The cells were lysed in ice-cold RIPA lysis buffer containing protease inhibitors (Beyotime Biotechnology, Shanghai, China). The protein concentration was determined using BCA™ Protein Assay Kit (Thermo Scientific, Rockford, USA). Equal amounts of protein were separated using SDS-PAGE and transferred to the polyvinylidene fluoride (PVDF) membrane. After blocking for 1 h, the membrane was incubated overnight at 4 °C with primary antibodies against the following proteins: mouse anti-proliferating cell nuclear antigen- (PCNA) (1:2000; Abcam), rabbit anti-Bcl-2 (1:2000; Abcam), rabbit anti-Caspase-3 (1:500; Abcam), rabbit anti-Caspase-8 (1:1000; Abcam), rabbit anti-Caspase-9 (1:2000; Abcam), rabbit anti-CD31(1:1000; Abcam), rabbit anti-phosphor-JNK (*p*-JNK) (1:1000, Cell Signaling Technology), rabbit anti-JNK (1:1000, Abcam), rabbit anti-PARP-1(1:1000; Abcam), rabbit anti-DFF40 (1:1000, Abcam) and rabbit anti- β-actin (1:5000; Abcam). The membrane was then probed with horseradish-peroxidase conjugated secondary antibody goat anti-rabbit IgG (1:2000; Abcam) or rabbit anti-mouse IgG (1:2000; Abcam) at room temperature for 1 h. The immunoreactive bands were visualised using an enhanced chemiluminescence (ECL) detection system.

2.9. Tube formation

Matrigel was dissolved at 4 °C overnight. Then, the thawed matrigel was added to a 12-well plate and incubated at 37 C for 30 min. Thereafter, 3×10^4 HUVECs and MHCC97-L cells were seeded on matrigel-coated 12-well plates and treated with 20 μg/ml, 40 μg/ml, and 200 μg/ml QACR or 3.72 μg/ml sorafenib. After 24h, the tube branches and length were analysed using ImageJ software (http://rsb.info.nih.gov/ij/).

2.10. Hematoxylin and eosin staining

Tumor tissues were fixed in a 10 % neutral formaldehyde, embedded in paraffin, and cut into 5 μm slices. After deparaffinisation and rehydration, sections were stained with hematoxylin and eosin (H&E) solution. Then, the cell morphology was observed using a light microscope (Olympus Corp.) equipped with an Olympus DP70 digital camera.

2.11. Immunohistochemical analysis

Formalin-fixed and paraffin-embedded tissue specimens were cut into thin 5 μm slices. The tissues were dewaxed and rehydrated using graded ethanol, followed by incubation at 4 °C overnight with primary antibodies against mouse anti-PCNA (1:10000; Abcam), rabbit anti-Bcl-2 (1:100; Abcam), rabbit anti-Caspase-3 (1:100; Abcam), rabbit anti-Caspase-8 (1:250; Abcam), rabbit anti-Caspase-9

(1:300; Abcam), rabbit anti-CD31 (1:250; Abcam), and rabbit anti-*p*-JNK (1:50; Cell Signaling Technology). The sections were washed with PBST and then incubated with secondary antibodies goat anti-rabbit IgG (1:1000; Abcam) or rabbit anti-mouse IgG (1:500; Abcam) at room temperature for 1 h. Protein expression was detected using the DAB Kit (Beyotime Biotechnology, Shanghai, China). At the same time, the nuclei were counterstained using hematoxylin (Sigma Aldrich, St. Louis, MO, USA). Images were captured using a light microscope (Olympus Corp.) with an Olympus DP70 digital camera.

2.12. Statistical analyses

All statistical analyses were performed using SPSS21.0 (SPSS Inc., Chicago, IL, USA). Data were expressed as the mean ± standard deviation (sd). Differences among multiple groups were analysed using a one-way or two-way analysis of variance (ANOVA). $P < 0.05$ was considered statistically significant.

3. Results

3.1. Qizhu Anti-Cancer Recipe suppresses the growth and angiopoiesis of anoikis-resistance hepatocellular carcinoma cells

To explorethe potential roles of QACR in anoikis-resistant HCC cells, we first detected the working concentrations of QACR by measuring the cell viability of Lx2 cells administrated with different doses of QACR, a notable reduction of cell viability was observed

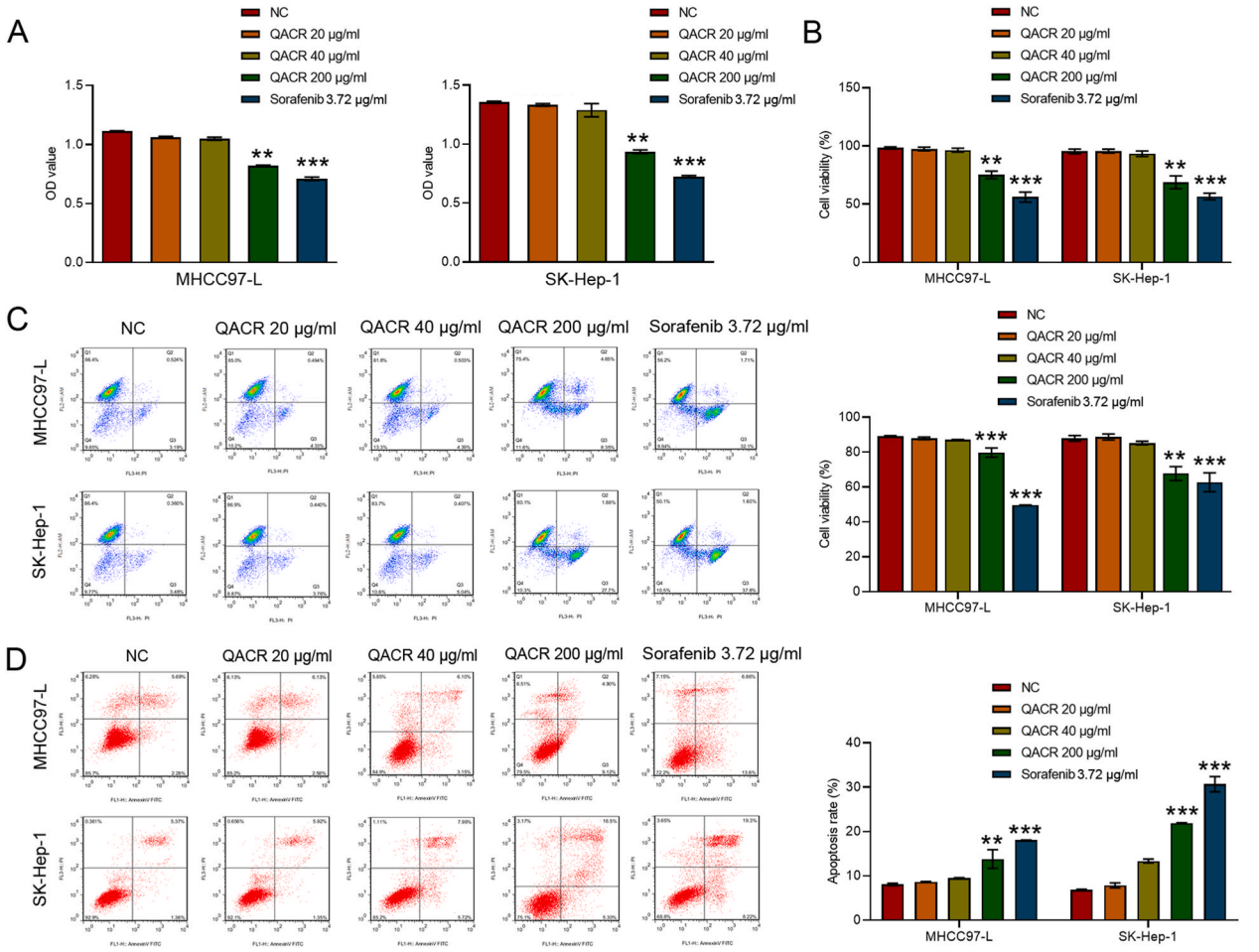

Fig. 1. The effects of Qizhu Anti-Cancer Recipe on anoikis-resistance hepatocellular carcinoma cell proliferation and apoptosis (A) Viable MHCC97-L and SK-Hep-1 cells treated with 3.72 μg/ml sorafenib or varying concentrations (0 μg/ml; 20 μg/ml; 40 μg/ml; 200 μg/ml) of Qizhu Anti-Cancer Recipe (QACR) in the ultra-low attachment 6-well plates according to cell counting kit 8 (CCK8) assay. (B) Viable cells in sorafenib or varying concentrations of QACR groups according to trypan blue assay. (C) Viable cells in sorafenib or varying concentrations of QACR groups according to calcein-AM/EthD-1 assay. (D) Cell apoptosis after sorafenib or varying concentrations of QACR treatment according to flow cytometry analysis with Annexin V/PI-staining. Data are presented as the mean ± SD of triplicate experiments, one-way ANOVA and two-way ANOVA were used for statistical test. Compared to the NC group, *P < 0.05, **P < 0.01, ***P < 0.001.

at 400 μg/ml (Supplementary Fig. 1A). Then MHCC97-L and SK-Hep-1 cells were treated with varying doses of QACR or sorafenib in the ultra-low attachment 6-well plates. As shown in Fig. 1A, sorafenib or QACR inhibited the growth of HCC cells. Furthermore, trypan blue exclusion assay revealed that QACR or sorafenib reduced the number of viable HCC cells (Fig. 1B). The inhibitory effect of sorafenib or QACR on the proliferation of anoikis-resistant HCC was further identified using calcein-AM/EthD-1 assay (Fig. 1C). The flow cytometry assay revealed that sorafenib or QACR significantly increased the apoptosis rate of HCC cells (Fig. 1D). Similar to cell growth and apoptosis results, sorafenib or QACR significantly reduced the expression of PCNA, Bcl-2, and CD31. At the same time, sorafenib or QACR significantly increased the expression of apoptosis-related proteins, including caspase-3, caspase-8, caspase-9, and DFF40 (Fig. 2A–G, Supplementary Fig. 1E). Next, the tube formation assay was performed to detect the effect of sorafenib or QACR on the angiopoiesis of anoikis-resistant HCC cells and HUVECs. The results showed that sorafenib or QACR reduced the angiogenesis of anoikis-resistant HCC cells and HUVECs (Fig. 2H). Our results suggested that QACR plays a role in the proliferation, apoptosis, and angiopoiesis of anoikis-resistant HCC cells.

3.2. *Qizhu Anti-Cancer Recipe suppresses the tumor progression in vivo*

Sorafenib or QACR was intragastrically administered to an orthotopic xenograft mouse model to validate further the anti-tumor effect of sorafenib or QACR on the growth of anoikis-resistant HCC cells *in vivo*. Compared with the control group, QACR treatment effectively inhibited tumor growth *in vivo* (Fig. 3A and B). Furthermore, the QACR treatment reduced the expression of the proliferation marker (PCNA and Bcl-2) and angiogenesis marker (CD31). At the same time, immunohistochemical analysis revealed that sorafenib or QACR treatment increased the expression of apoptosis markers, including caspase-3, caspase-8, and caspase-9 (Fig. 3C and D). Consistent with the results from the immunohistochemical analysis, the expression of PCNA, Bcl-2, and CD31 was downregulated

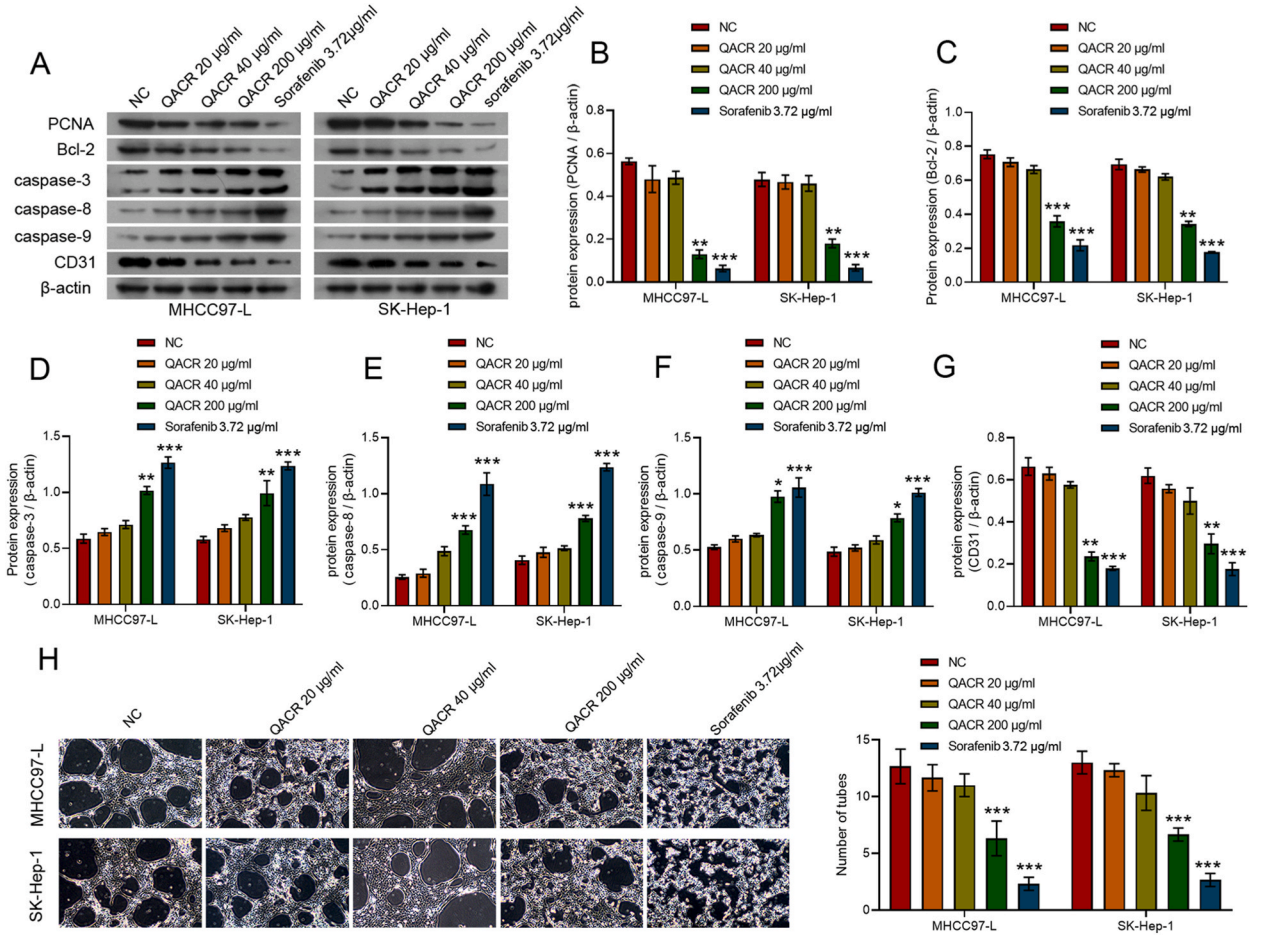

Fig. 2. The effects of Qizhu Anti-Cancer Recipe on apoptotic proteins and angiopoiesis in hepatocellular carcinoma cells. (A–G) The effects of 3.72 μg/ml sorafenib or QACR (0 μg/ml; 20 μg/ml; 40 μg/ml; 200 μg/ml) on the expression of proliferating cell nuclear antigen (PCNA), Bcl-2, caspase-3, caspase-8, caspase-9, and CD31 according to Western blot analysis. (H) Angiogenesis in MHCC97-L or SK-Hep-1 cells and HUVECs according to tube formation assay. Data are presented as the mean ± SD of triplicate experiments, one-way ANOVA and two-way ANOVA were used for statistical test. Compared to the NC group,*P < 0.05, **P < 0.01, ***P < 0.001.

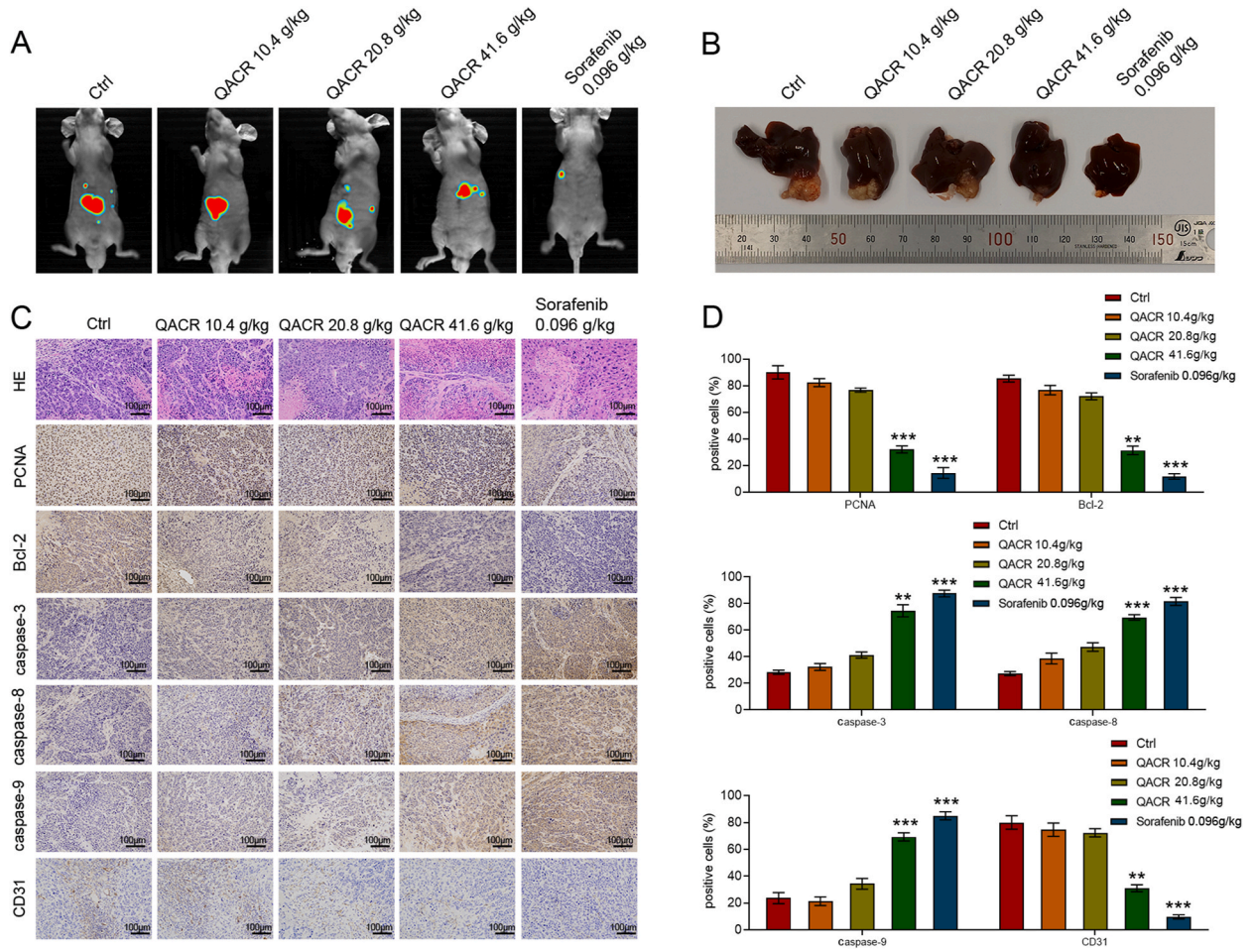

Fig. 3. The effects of Qizhu Anti-Cancer Recipe on tumor growth and angiopoiesis *in vivo* (A) The effects of QACR (0 g/kg; 10.4 g/kg; 20.8 g/kg; 41.6 g/kg) *in vivo* tumor growth according to Bioluminescence imaging. (B) Representative image of liver tumor obtained from mice in each group. (C) The expression of PCNA, Bcl-2, CD31, caspase-3, caspase-8, and caspase-9 in each group according to immunohistochemical analysis. (D) The positive rate of PCNA, Bcl-2, CD31, caspase-3, caspase-8, CD31, and caspase-9 in each group. Data are presented as the mean ± SD of five independent experiments, one-way ANOVA was used for statistical test. Compared to the control group,*P < 0.05, **P < 0.01, ***P < 0.001.

in the sorafenib or QACR group. At the same time, the expression of caspase-3, caspase-8, caspase-9, DFF40 was upregulated in the sorafenib or QACR (Fig. 4A–D, Supplementary Fig. 1F). Based on the above results, QACR inhibits the progression of HCC *in vivo*.

3.3. Qizhu Anti-Cancer Recipe modulates the c-Jun N-terminal kinase pathway

The stress-activated c-JUN NH2-terminal kinase (JNK) pathway plays a crucial role in cell anoikis, growth, and tube formation [20–22]. Previous Studies have reported that the JNK pathway plays a role in the development and progression of several cancers [23]. Therefore, we hypothesised that sorafenib or QACR regulates the JNK pathway. We examined the JNK pathway in HCC tumor tissues to validate this hypothesis using the immunohistochemical and Western blot analysis. As shown in Fig. 5A, 0.096 g/kg of sorafenib or 41.6 g/kg of QACR treatment increased the positive rate of *p*-JNK. Western blot (Fig. 5B) and Elisa analysis (Supplementary Fig. 1B) revealed similar results. Western blot and Elisa assays were performed to validate whether sorafenib or QACR impacts the protein levels of the JNK pathway in anoikis-resistant HCC cells. Consistent with the above results, QACR administration with concentration of 200 μg/ml dramatically upregulated the expression of *p*-JNK (Fig. 5C, Supplementary Figs. 1C and 1D). In summary, these data validated that QACR could modulate the expression of *p*-JNK in hepatocellular carcinoma cells.

3.4. SP600125 reversed the inhibitory effects of Qizhu Anti-Cancer Recipe on the growth and angiopoiesis of anoikis-resistance hepatocellular carcinoma cells

We designed rescue experiments to clarify whether sorafenib or QACR suppresses the anoikis resistance, growth of HCC cells, and tube formation of anoikis-resistant HCC cells by the activation of the JNK signaling pathway. As shown by Western blot, SP600125 (10

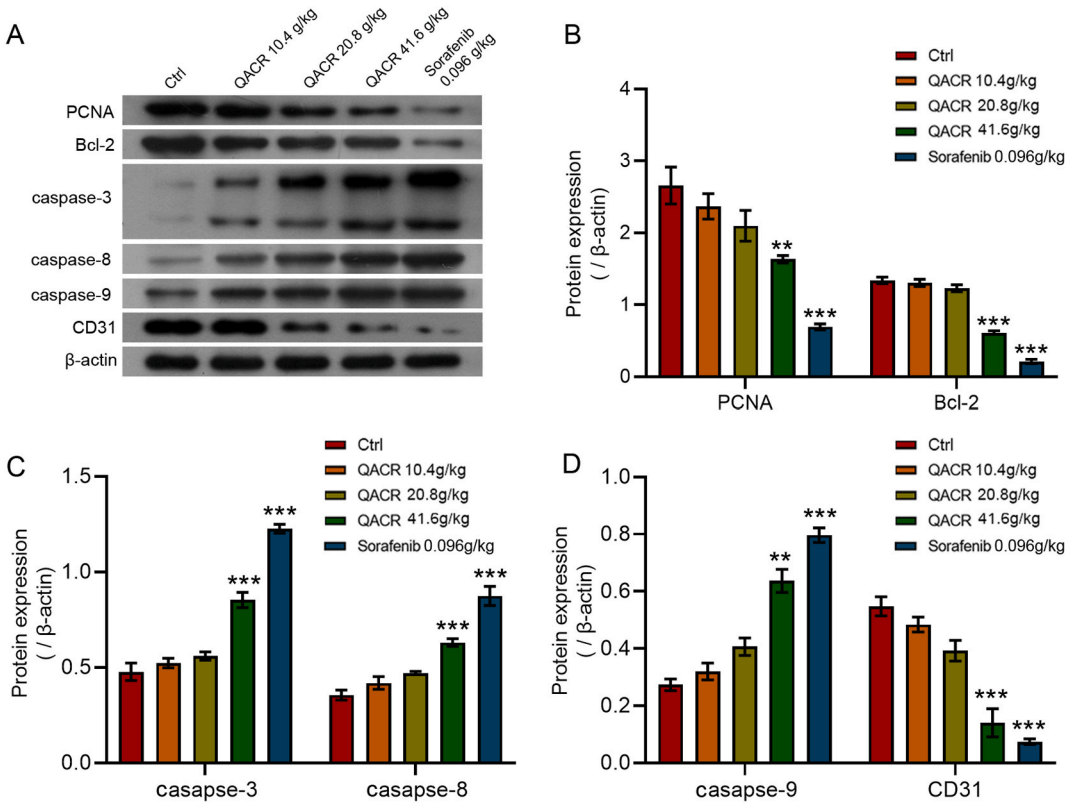

Fig. 4. The effects of Qizhu Anti-Cancer Recipe on proliferation, apoptosis, angiopoiesis -related proteins *in* vivo (A) The expression of PCNA, Bcl-2, CD31, caspase-3, caspase-8, and caspase-9 in tumor tissues obtained from each group according to Western blot. (B–D) The densitometry analysis of PCNA, Bcl-2, CD31, caspase-3, caspase-8, and caspase-9. Data are presented as the mean ± SD of five independent experiments, one-way ANOVA was used for statistical test. Compared to the control group,*P < 0.05, **P < 0.01, ***P < 0.001.

μM), a c-Jun N-terminal kinase inhibitor, successfully reversed the expression of *p*-JNK increased after sorafenib (3.72 μg/ml) or QACR (200 μg/ml) treatment (Fig. 6A). CCK-8 and Trypan blue assays revealed that SP600125 significantly increased the number of viable cells after sorafenib or QACR treatment (Fig. 6B and C). These findings were further validated using calcein-AM/EthD-1 analysis (Fig. 6D). In addition, SP600125 effectively inhibited cell apoptosis after sorafenib or QACR treatment (Fig. 6E). Furthermore, SP600125 enhanced tube formation inhibited in the sorafenib or QACR group (Fig. 6F). Consistent with the above results, SP600125 reversed the inhibited expression of PCNA, Bcl-2, and CD31 and the enhanced expression of caspase-3, caspase-8, caspase-9, and DFF40 induced by sorafenib or QACR (Fig. 6G, Supplementary Fig. 1G). Taken together, the JNK inhibitor could regulate the proliferation, apoptosis, and tube formation of anoikis-resistance hepatocellular carcinoma cells impacted after QACR treatment.

4. Discussion

JNK pathway plays critical roles in cell death, survival, differentiation, proliferation, and tumorigenesis in hepatocytes [24–26]. In this research, we found that QACR can remarkably restrain the proliferation, metastasis, and angiopoiesis in anoikis-resistant HCC cells and BALB/c nude mice by activating the JNK pathway. And the inhibitory effects of QACR in liver cancer was markedly reversed by administration with JNK inhibitor.

As a traditional Chinese medicine (TCM), the main ingredients of QACR including Bupleurum root, Radix Paeoniae Alba, and Rhizoma zedoariae have been demonstrated to nourish blood and liver and been broadly utilized for treating several liver diseases in eastern Asian countries [27,28]. Several active compounds of QACR including oleanolic acid, asperulosidic acid, ononin, daidzein, formononetin have been reported to exert significant hepatoprotective effects. For example, oleanolic acid suppressed the migration and invasion of the liver cancer cells via regulating of the JNK/p38 signalling pathway [29]. Asperulosidic acid restrains hepatocellular carcinoma development and enhances chemosensitivity through inactivating the MEKK1/NF-κB pathway [30]. Moreover, ononin, daidzein, formononetin were identified as active compounds in TCM that affect the development of liver fibrosis by regulating inflammation, immunity, angiogenesis, antioxidants [31]. The underlying mechanisms might be related to their effects of inhibiting proliferation, inflammation and angiogenesis. In this study, we first explored the inhibitory effects of QACR on anoikis-resistant HCC cells and mice model. It was discovered that QACR treatment effectively restrained the proliferation and angiopoiesis of anoikis-resistant HCC cells *in vitro* as well as the tumor growth *in vivo*, while promoting the apoptosis, which were in consistent with the

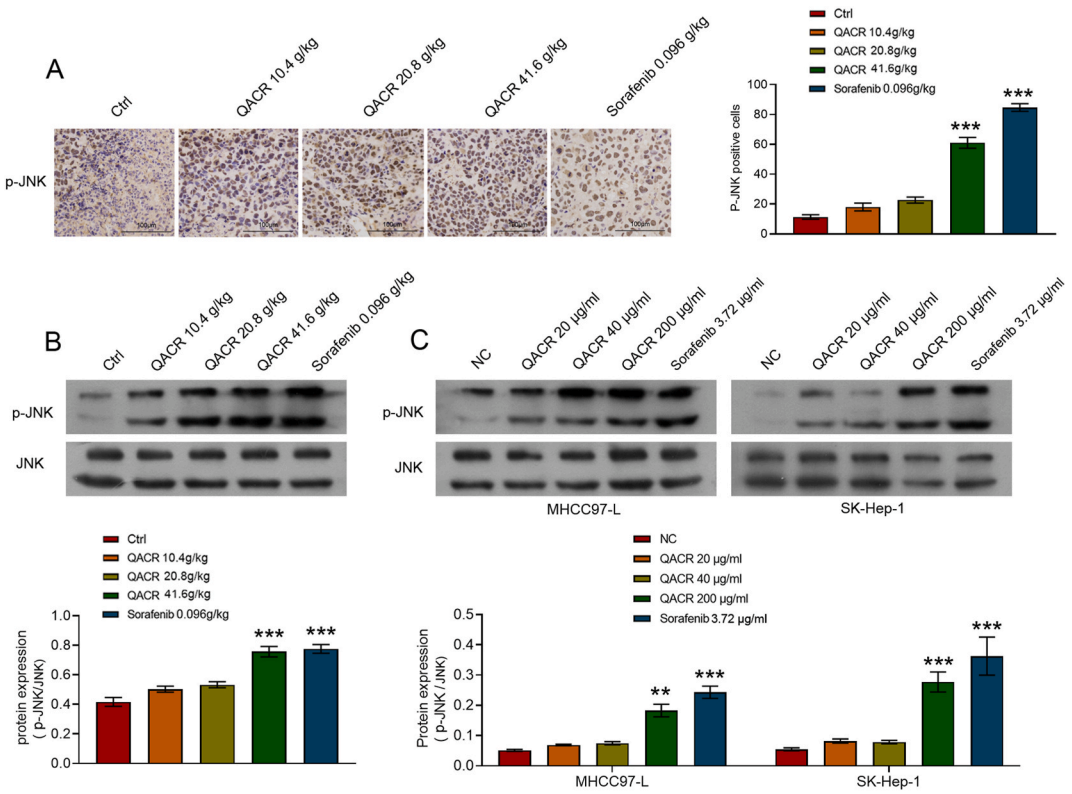

Fig. 5. The effects of Qizhu Anti-Cancer Recipe on the c-Jun N-terminal kinase pathway (A–B) Immunohistochemical and Western blot analysis of phospho-*c*-Jun NH2-terminal kinase (*p*-JNK) protein expression in tumors from each group. (C) The expression of *p*-JNK in anoikis-resistance MHCC97-L and SK-Hep-1 cells treated with sorafenib or varying concentrations of QACR according to Western blot. For cell experiments, data are reported as the mean ± SD of three experiments, while for animal experiments, data are presented as the mean ± SD of five independent experiments. one-way ANOVA and two-way ANOVA were used for statistical test. Compared to the NC or control group,*P < 0.05, **P < 0.01, ***P < 0.001.

previous findings. Anoikis could impede detached cells from reattaching to new matrices and developing dysplasia [32]. Resistance to anoikis, an important step in metastasis, promotes the survival of cancer cells while migrating to secondary sites [3]. Therefore, it is critical to understand the cellular characteristics and molecular mechanisms of anoikis in HCC, which could be helpful with the development of therapy and prognosis of HCC. We are the first to investigate the effects of the QACR on the proliferation and apoptosis of anoikis-resistant HCC both *in vivo* and *in vitro*. Flow cytometry analysis indicated that QACR significantly increased the apoptosis rate of HCC cells, and the expression of apoptosis-related proteins, including caspase-3, caspase-8, caspase-9, PARP-1, DFF40, were markedly changed, indicating that QACR can activate the cell apoptosis in anoikis-resistant HCC cells.

The c-Jun N-terminal kinases (JNKs), members of the mitogen-activated protein kinase (MAPK) family, regulates various physiological processes, including cell proliferation, survival, death, DNA repair, metabolism, anoikis, and angiogenesis [3,33,34]. Here, we found that QACR administration upregulated the expression of *p*-JNK in anoikis-resistant HCC cells and tumor tissues. Moreover, the addition of SP600125 reversed the positive effects of QACR on inhibiting the HCC cell proliferation, tube formation as well as tumor growth. These results suggested that the inhibitory effects of QACR in liver cancer are connected with the regulation of JNK signaling.

In conclusion, QACR can inhibit the anoikis-resistant HCC cells proliferation and tumors growth, and might exert this effect by regulating the JNK pathway, suggesting that QACR may serve as a new therapeutic strategy in HCC.

Financial support

This work was supported by Shenzhen Science and Technology Project (NO. JCYJ20180302173542393, JCYJ20210324120405015).

Ethics approval and consent to participate

All animal studies were conducted in accordance with the ARRIVE guidelines. All *in vivo* experiments were performed according to the Care and Use of Laboratory Animals guidelines of Peking University Shenzhen Graduate School and approved by the Institutional Animal Care and Use Committee (IACUC) of Peking University Shenzhen Graduate School (Approval No. 92153).

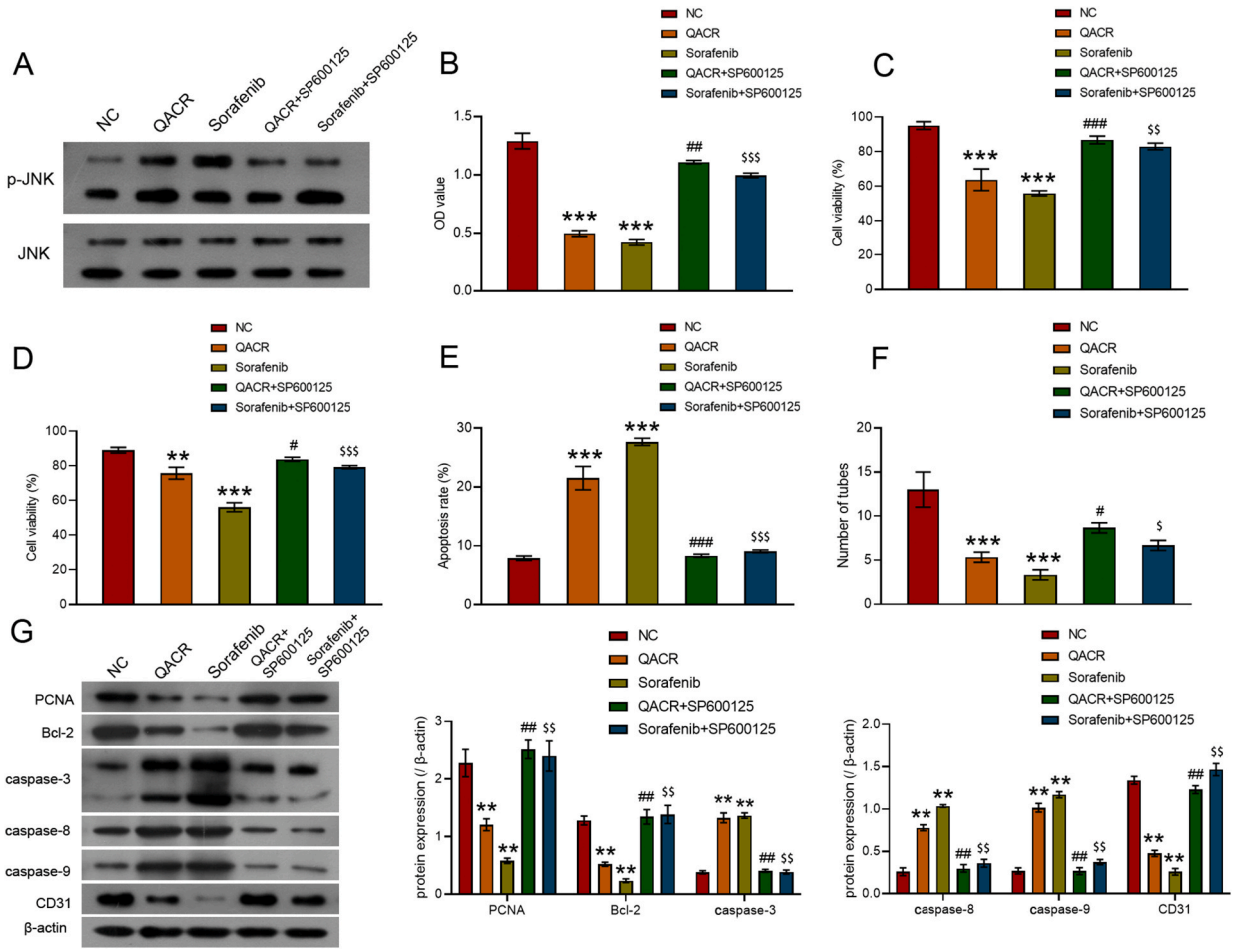

Fig. 6. The association between c-Jun N-terminal kinase inhibitor SP600125 and Qizhu Anti-Cancer Recipe in regulating the growth and angiopoiesis of anoikis-resistance hepatocellular carcinoma cells (A) The effects of SP600125 (10 μM) on anoikis-resistance MHCC97-L after sorafenib (3.72 μg/ml) or QACR (200 μg/ml) treatment. The expression of *p*-JNK was detected using Western blot. (B–G) Growth and angiopoiesis of Anoikis-resistance HCC cells according to CCK8, trypan blue, calcein-AM/EthD-1, flow cytometry, Tube formation, and Western blot assays, respectively. Data are presented as the mean ± SD of triplicate experiments, one-way ANOVA was used for statistical test. Compared to the NC group, $^{*}P < 0.05$, $^{**}P < 0.01$, $^{***}P < 0.001$; Compared to the QACR group, $^{\#}P < 0.05$, $^{\#\#}P < 0.01$, $^{\#\#\#}P < 0.001$; Compared to the sorafenib group, $^{\$}P < 0.05$, $^{\$}\$P < 0.01$, $^{\$\$\$}P < 0.001$.

Data availability statement

Data will be made available on request.

CRediT authorship contribution statement

Zhiyi Han: Writing – original draft, Project administration, Methodology. **Qi Huang:** Software. **Minling Lv:** Formal analysis, Data curation. **Mengqing Ma:** Investigation. **Wei Zhang:** Visualization. **Wenxing Feng:** Software, Resources. **Rui Hu:** Validation. **Xinfeng Sun:** Validation. **Jing Li:** Software. **Xin Zhong:** Formal analysis. **Xiaozhou Zhou:** Writing – review & editing, Funding acquisition, Conceptualization.

Declaration of competing interest

The authors declare that they have no known competing financial interests or personal relationships that could have appeared to influence the work reported in this paper.

Appendix A. Supplementary data

Supplementary data to this article can be found online at https://doi.org/10.1016/j.heliyon.2023.e22089.

References

[1] D.W. Kim, C. Talati, R. Kim, Hepatocellular carcinoma (HCC): beyond sorafenib-chemotherapy, J. Gastrointest. Oncol. 8 (2) (2017) 256–265, https://doi.org/10.21037/jgo.2016.09.07.

[2] H. Sung, J. Ferlay, R.L. Siegel, et al., Global cancer Statistics 2020: GLOBOCAN estimates of incidence and mortality worldwide for 36 cancers in 185 countries, CA Cancer J. Clin. 71 (3) (2021) 209–249, https://doi.org/10.3322/caac.21660.

[3] B. Sun, C. Hu, Z. Yang, et al., Midkine promotes hepatocellular carcinoma metastasis by elevating anoikis resistance of circulating tumor cells, Oncotarget 8 (20) (2017) 32523–32535, https://doi.org/10.18632/oncotarget.15808.

[4] L. Liu, H. Jiang, H. Pan, et al., LncRNA XIST promotes liver cancer progression by acting as a molecular sponge of miR-200b-3p to regulate ZEB1/2 expression, J. Int. Med. Res. 49 (5) (2021), 3000605211016211, https://doi.org/10.1177/03000605211016211.

[5] P. Paoli, E. Giannoni, P. Chiarugi, Anoikis molecular pathways and its role in cancer progression, Biochim. Biophys. Acta 1833 (12) (2013) 3481–3498, https://doi.org/10.1016/j.bbamcr.2013.06.026.

[6] Y.N. Kim, K.H. Koo, J.Y. Sung, et al., Anoikis resistance: an essential prerequisite for tumor metastasis, Int. J. Cell Biol. 2012 (2012), 306879, https://doi.org/10.1155/2012/306879.

[7] H.Y. Lee, S.W. Son, S. Moeng, et al., The role of noncoding RNAs in the regulation of anoikis and anchorage-independent growth in cancer, Int. J. Mol. Sci. 22 (2) (2021), https://doi.org/10.3390/ijms22020627.

[8] J. Song, Y. Liu, F. Liu, et al., The 14-3-3sigma protein promotes HCC anoikis resistance by inhibiting EGFR degradation and thereby activating the EGFR-dependent ERK1/2 signaling pathway, Theranostics 11 (3) (2021) 996–1015, https://doi.org/10.7150/thno.51646.

[9] Z. Gao, G.S. Zhao, Y. Lv, et al., Anoikis-resistant human osteosarcoma cells display significant angiogenesis by activating the Src kinase-mediated MAPK pathway, Oncol. Rep. 41 (1) (2019) 235–245, https://doi.org/10.3892/or.2018.6827.

[10] G.M. Keating, Sorafenib: a review in hepatocellular carcinoma, Target Oncol. 12 (2) (2017) 243–253, https://doi.org/10.1007/s11523-017-0484-7.

[11] S. Lin, K. Hoffmann, C. Gao, et al., Melatonin promotes sorafenib-induced apoptosis through synergistic activation of JNK/c-jun pathway in human hepatocellular carcinoma, J. Pineal Res. 62 (3) (2017), https://doi.org/10.1111/jpi.12398.

[12] J.M. Llovet, S. Ricci, V. Mazzaferro, et al., Sorafenib in advanced hepatocellular carcinoma, N. Engl. J. Med. 359 (4) (2008) 378–390, https://doi.org/10.1056/NEJMoa0708857.

[13] Y. Zhang, Y. Lou, J. Wang, et al., Research status and molecular mechanism of the traditional Chinese medicine and antitumor therapy combined strategy based on tumor microenvironment, Front. Immunol. 11 (2020), 609705, https://doi.org/10.3389/fimmu.2020.609705.

[14] T.H. So, S.K. Chan, V.H. Lee, et al., Chinese medicine in cancer treatment - how is it practised in the east and the west? Clin. Oncol. 31 (8) (2019) 578–588, https://doi.org/10.1016/j.clon.2019.05.016.

[15] J. Zhang, L. Guo, X. Zhou, et al., Dihydroartemisinin induces endothelial cell anoikis through the activation of the JNK signaling pathway, Oncol. Lett. 12 (3) (2016) 1896–1900, https://doi.org/10.3892/ol.2016.4870.

[16] L.F. Wan, J.J. Shen, Y.H. Wang, et al., Extracts of Qizhu decoction inhibit hepatitis and hepatocellular carcinoma in vitro and in C57BL/6 mice by suppressing NF-kappaB signaling, Sci. Rep. 9 (1) (2019) 1415, https://doi.org/10.1038/s41598-018-38391-9.

[17] F. Yang, M. Li, D. Xu, et al., Inhibition of JNK/c-Jun-ATF2 overcomes cisplatin resistance in liver cancer through down-regulating galectin-1, Int. J. Biol. Sci. 19 (8) (2023) 2366–2381, https://doi.org/10.7150/ijbs.79163.

[18] L. Xu, W. Wang, T. Meng, et al., New microtubulin inhibitor MT189 suppresses angiogenesis via the JNK-VEGF/VEGFR2 signaling axis, Cancer Lett. 416 (2018) 57–65, https://doi.org/10.1016/j.canlet.2017.12.022.

[19] Y.J. Chen, C.D. Kuo, Y.M. Tsai, et al., Norcantharidin induces anoikis through Jun-N-terminal kinase activation in CT26 colorectal cancer cells, Anti Cancer Drugs 19 (1) (2008) 55–64, https://doi.org/10.1097/CAD.0b013e3282f18826.

[20] Z. Huang, Y. Xia, K. Hu, et al., Histone deacetylase 6 promotes growth of glioblastoma through the MKK7/JNK/c-Jun signaling pathway, J. Neurochem. 152 (2) (2020) 221–234, https://doi.org/10.1111/jnc.14849.

[21] N. Girnius, R.J. Davis, JNK promotes epithelial cell anoikis by transcriptional and post-translational regulation of BH3-only proteins, Cell Rep. 21 (7) (2017) 1910–1921, https://doi.org/10.1016/j.celrep.2017.10.067.

[22] C.Y. Changchien, H.H. Chang, M.S. Dai, et al., Distinct JNK/VEGFR signaling on angiogenesis of breast cancer-associated pleural fluid based on hormone receptor status, Cancer Sci. 112 (2) (2021) 781–791, https://doi.org/10.1111/cas.14772.

[23] C. Bubici, S. Papa, JNK signalling in cancer: in need of new, smarter therapeutic targets, Br. J. Pharmacol. 171 (1) (2014) 24–37, https://doi.org/10.1111/bph.12432.

[24] P. Piccolo, R. Ferriero, A. Barbato, et al., Up-regulation of miR-34b/c by JNK and FOXO3 protects from liver fibrosis, Proc. Natl. Acad. Sci. U.S.A. 118 (10) (2021), https://doi.org/10.1073/pnas.2025242118.

[25] D. Xie, H. Zhao, J. Lu, et al., High uric acid induces liver fat accumulation via ROS/JNK/AP-1 signaling, Am. J. Physiol. Endocrinol. Metab. 320 (6) (2021) E1032–E1043, https://doi.org/10.1152/ajpendo.00518.2020.

[26] S. Torres, A. Baulies, N. Insausti-Urkia, et al., Endoplasmic reticulum stress-induced upregulation of STARD1 promotes acetaminophen-induced acute liver failure, Gastroenterology 157 (2) (2019) 552–568, https://doi.org/10.1053/j.gastro.2019.04.023.

[27] G. Cao, Q. Li, H. Cai, et al., Investigation of the chemical changes from crude and processed Paeoniae Radix alba-atractylodis macrocephalae rhizoma herbal pair extracts by using Q exactive high-performance benchtop quadrupole-orbitrap LC-MS/MS, Evid. Based Complement Alternat. Med. 2014 (2014), 170959, https://doi.org/10.1155/2014/170959.

[28] A. Liu, N. Tanaka, L. Sun, et al., Saikosaponin d protects against acetaminophen-induced hepatotoxicity by inhibiting NF-kappaB and STAT3 signaling, Chem. Biol. Interact. 223 (2014) 80–86, https://doi.org/10.1016/j.cbi.2014.09.012.

[29] C. Gao, X. Li, S. Yu, et al., Inhibition of cancer cell growth by oleanolic acid in multidrug resistant liver carcinoma is mediated via suppression of cancer cell migration and invasion, mitochondrial apoptosis, G2/M cell cycle arrest and deactivation of JNK/p38 signalling pathway, J. BUON 24 (5) (2019) 1964–1969.

[30] L. Li, H. Qiu, Asperulosidic acid restrains hepatocellular carcinoma development and enhances chemosensitivity through inactivating the MEKK1/NF-kappaB pathway, Appl. Biochem. Biotechnol. (2023), https://doi.org/10.1007/s12010-023-04500-2.

[31] Q. Zhao, J. Bai, Y. Chen, et al., An optimized herbal combination for the treatment of liver fibrosis: hub genes, bioactive ingredients, and molecular mechanisms, J. Ethnopharmacol. 297 (2022), 115567, https://doi.org/10.1016/j.jep.2022.115567.

[32] F.O. Adeshakin, A.O. Adeshakin, L.O. Afolabi, et al., Mechanisms for modulating anoikis resistance in cancer and the relevance of metabolic reprogramming, Front. Oncol. 11 (2021), 626577, https://doi.org/10.3389/fonc.2021.626577.

[33] W. Gao, R. He, J. Ren, et al., Exosomal HMGB1 derived from hypoxia-conditioned bone marrow mesenchymal stem cells increases angiogenesis via the JNK/HIF-1alpha pathway, FEBS Open Bio 11 (5) (2021) 1364–1373, https://doi.org/10.1002/2211-5463.13142.

[34] A. Zeke, M. Misheva, A. Remenyi, et al., JNK signaling: regulation and functions based on complex protein-protein partnerships, Microbiol. Mol. Biol. Rev. 80 (3) (2016) 793–835, https://doi.org/10.1128/MMBR.00043-14.